Guanidine Complexes of Platinum: A Theoretical Study

ARTICLE *in* THE JOURNAL OF PHYSICAL CHEMISTRY A · JULY 2014

Impact Factor: 2.69 · DOI: 10.1021/jp504483x · Source: PubMed

4 AUTHORS, INCLUDING:

Marta Marin-Luna
University of Vigo
29 PUBLICATIONS **111** CITATIONS
SEE PROFILE

Goar Sánchez
University College Dublin
69 PUBLICATIONS **905** CITATIONS
SEE PROFILE

Patrick O'Sullivan
Trinity College Dublin
2 PUBLICATIONS **1** CITATION
SEE PROFILE

THE JOURNAL OF PHYSICAL CHEMISTRY A

Article

pubs.acs.org/JPCA

Guanidine Complexes of Platinum: A Theoretical Study

Marta Marin-Luna,[†] Goar Sanchez-Sanz,[‡] Patrick O'Sullivan,[§] and Isabel Rozas*[,§]

[†]Departamento de Química Orgánica, Universidad de Murcia, Facultad de Química, Regional Campus of International Excellence "Campus Mare Nostrum", Espinardo, 30100 Murcia, Spain

[‡]School of Physics & Complex and Adaptive Systems Laboratory, University College Dublin, Belfield, Dublin 4, Ireland

[§]School of Chemistry, Trinity Biomedical Sciences Institute, Trinity College Dublin, 152-160 Pearse Street, Dublin 2, Ireland

Supporting Information

ABSTRACT: We have studied theoretically the complexes of model *N*-phenylguanidine/ium derivatives with $PtCl_3^-$ and $PtCl_2$ in different coordinating modes (mono- and bidentate) with different N atoms of the guanidine/ium moiety using the B3LYP/6-31+G** and LANL2DZ mixed basis set. This will aid the understanding of the complexation between platinum and the guanidine or guanidinium moiety in order to design dual anticancer agents that combine a guanidine-based DNA minor groove binder and a cisplatin-like moiety. Calculated interaction and relative energies, analysis of the electron density, and examination of the orbital interactions indicate that the most stable type of complex is that with a monodentate interaction between $PtCl_3^-$ and guanidinium established through one of the NH_2 groups. Next, we optimized the structure of three *bis*-guanidinium diaromatic systems developed in our group as DNA minor groove binders and their complexation with $PtCl_3^-$, finding that the formation of Pt complexes of these minor groove binders is favorable and would produce stable monodentate coordinated systems.

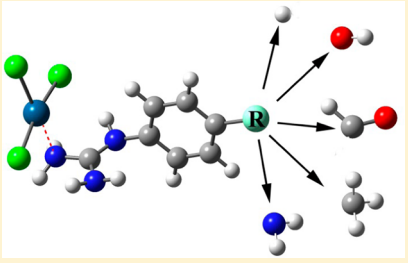

INTRODUCTION

After the discovery of cisplatin as an antitumor drug, different Pt compounds were developed, and now almost 50% of all anticancer therapies are Pt-based.[1] However, only three of these Pt-based drugs are used worldwide in the clinical setting,[2] and considering that multifactorial resistance and severe toxicity have limited their use, there is a real need for more potent Pt drugs with less toxicity and resistance. Different Pt drugs have been prepared, and their DNA interaction has been studied,[3] yielding good cytotoxicity results.[4−7] Some of these Pt drugs are dual-action drugs, for example, the Pt complex of a histone deacetylase inhibitor developed by Marmion.[8]

A different approach to new dual-action antineoplastic metallodrugs could be the use of Pt complexes of well-known DNA-targeting agents such as minor groove binders (MGB). Rozas's group has already prepared symmetric and asymmetric guanidine-like dications[9] that strongly interact with DNA as MGBs (such as compounds **1**−**4** shown in Figure 1), according to different biophysical experiments such as UV titrations, DNA thermal denaturation, circular and linear dichroism (CD and LD), isothermal calorimetry (ITC), and surface plasmon resonance (SPR).[10−12]

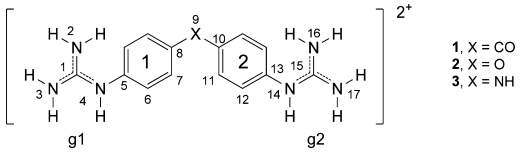

Figure 1. Examples of *bis*-guanidinium systems previously prepared by Rozas and co-workers. Atom numbering and group names used in the text are indicated.

Several examples of Pt-based DNA-targeting drugs, mostly using intercalating thioureas, have been recently published.[13,14] The use of these bifunctional small molecules is strongly supported by Crews et al.[15] as a new strategy for developing selective and specific therapeutics. In this sense, we propose that potential Pt-MGB complexes could be very effective chemotherapeutics, and our hypothesis is that they will first interact with the minor groove of genomic DNA (by means of the MGB moiety) bringing near the Pt moiety, which then will bind to the DNA bases in a cisplatin manner.

The computational study of complexes of hydrazine, group 10 metals such as Ni, Pd or Pt, and halogen atoms using density functional theory and the LANL2DZ pseudopotential has been previously described in the literature.[16] This study showed that the M−N bonds are formed by the electron lone pair of the N atom and a contribution from the metal atom, indicating covalency of the bonds. This same group later published a theoretical study of square planar complexes formed by different difluoro 2,2′-bipyridines and two $M-X_2$ (M = Pd or Pt and X = F, Cl, Br, or I) fragments using the same level of computation and found several interesting relationships between the chiral distinction energy and the different moieties.[17] All this work encouraged us to computationally study a number of monodentate and bidentate Pt complexes

Received: May 7, 2014
Revised: June 25, 2014
Published: July 2, 2014

dx.doi.org/10.1021/jp504483x | *J. Phys. Chem. A* 2014, 118, 5540−5547

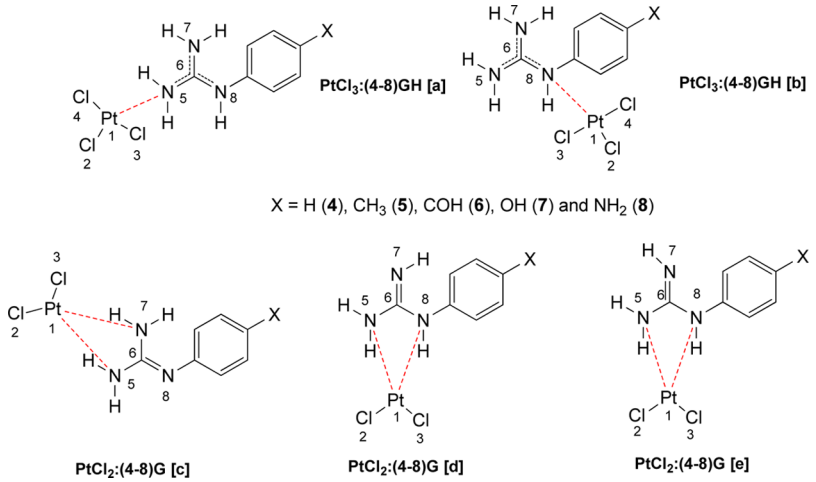

Figure 2. Structure and numbering of the Pt complexes of the *N*-arylguanidines/iums (**4**−**8**) studied in this work. GH, guanidinium; G, guanidine; $PtCl_3^-$, monodentate; $PtCl_2$, bidentate.

with *N*-arylguanidine/ium systems **4**−**8** (Figure 2) in order to understand the interaction between Pt and guanidine or its cation.

COMPUTATIONAL METHODS

The density functional theory (DFT) and Becke's three-parameter functional and the Lee−Yang−Parr[18] (B3LYP) functional level, as implemented in the Gaussian 09 package,[19] have been employed to optimize all of the geometries. Additionally, the "double-ξ" LANL2DZ basis set consisting of 18 valence electrons associated with the effective core potentials (ECPs) of Hay and Wadt[20,21] has been employed for Pt atoms, and the 6-31+G** basis set[22] has been used for hydrogen, carbon, oxygen, nitrogen, and chlorine atoms. The solvent effect of water was taken into account using the polarizable continuum model (PCM). Net atomic charges have been obtained using the natural bond orbital (NBO)[23] analysis of Weinhold and Carpenter using the NBO-3 program and analyzed charge-transfer and orbital interactions between occupied and unoccupied orbitals. The atoms in molecules (AIM) methodology[24,25] was used to analyze the electron density of the systems with the AIMAll program.[26]

RESULTS AND DISCUSSION

Platinum Complexes of Monoguanidine/Guanidinium Derivatives. Before attempting the study of the platinum complexes with the guanidine/ium groups of compounds **1**−**3**, we have studied a series of *N*-phenylguanidine or *N*-phenylguanidinium derivatives bearing a substituent (X = H, CH_3, CHO, OH, or NH_2) in the *para* position (compounds **4**−**8**, respectively) as models. We have defined five types of complexes based on the established interactions (Figure 2): monodentate guanidinium complexes type [**a**] in which the main metal−ligand interaction is formed with one of the NH_2 groups of the cation; monodentate guanidinium complexes type [**b**] in which the coordinative bond is established with the exocyclic NH group of the cation; guanidine bidentate complexes type [**c**] formed by two Pt−N coordinative bonds with two NH_2 groups of guanidine; and finally, the guanidine bidentate complexes types [**d**] and [**e**] in which the interaction with the Pt atom is formed by the exocyclic NH and the NH_2 groups of the guanidine group. These last complex types are different in the orientation of the hydrogen atom at the NH group not involved in complexation: in complex type [**d**], the hydrogen atom is "in" (close to the phenyl ring), whereas in complex type [**e**], the same hydrogen atom is "out" (far from the phenyl ring).

Table 1. Interaction Energy (E_I, kJ mol^{-1}) and Relative Energy Difference (ΔE_R, kJ mol^{-1}) Calculated for the $PtCl_3$:(4−8)GH [a,b] and $PtCl_2$:(4−8)G [c−e] Complexes Studied at the B3LYP/6-31+G and LANL2DZ Mixed Basis Set, in the Gas Phase**

complex	X	E_I	ΔE_R
$PtCl_3$:4GH [a]	H	−342.5	−43.5
$PtCl_3$:5GH [a]	CH_3	−336.4	−37.4
$PtCl_3$:6GH [a]	CHO	**−349.8**	**−50.8**
$PtCl_3$:7GH [a]	OH	−338.7	−39.7
$PtCl_3$:8GH [a]	NH_2	−327.3	−28.4
$PtCl_3$:4GH [b]	H	−315.3	−16.3
$PtCl_3$:5GH [b]	CH_3	−309.2	−10.2
$PtCl_3$:6GH [b]	CHO	−323.8	−24.8
$PtCl_3$:7GH [b]	OH	−312.1	−13.1
$PtCl_3$:8GH [b]	NH_2	−299.0	0.0
$PtCl_2$:4G [c]	H	−160.0	−24.9
$PtCl_2$:5G [c]	CH_3	−161.9	−26.8
$PtCl_2$:6G [c]	CHO	−139.7	−4.6
$PtCl_2$:7G [c]	OH	−162.3	−27.2
$PtCl_2$:8G [c]	NH_2	−170.0	−34.9
$PtCl_2$:4G [d]	H	−164.5	−29.4
$PtCl_2$:5G [d]	CH_3	−166.2	−31.1
$PtCl_2$:6G [d]	CHO	−145.2	−10.1
$PtCl_2$:7G [d]	OH	−168.8	−33.7
$PtCl_2$:8G [d]	NH_2	**−172.4**	**−37.3**
$PtCl_2$:4G [e]	H	−154.2	−19.1
$PtCl_2$:5G [e]	CH_3	−155.6	−20.5
$PtCl_2$:6G [e]	CHO	−135.1	0.0
$PtCl_2$:7G [e]	OH	−159.1	−24.0
$PtCl_2$:8G [e]	NH_2	−162.1	−27.0

Considering that all the Pt complexes studied present zero formal charge, in the monodentate complexes (type [**a**] or [**b**]) three chlorine atoms complete the coordination sphere of platinum atom, whereas in the bidentate complexes (type [**c**], [**d**], or [**e**]) two chlorine atoms are present. The optimized

dx.doi.org/10.1021/jp504483x | J. Phys. Chem. A 2014, 118, 5540−5547

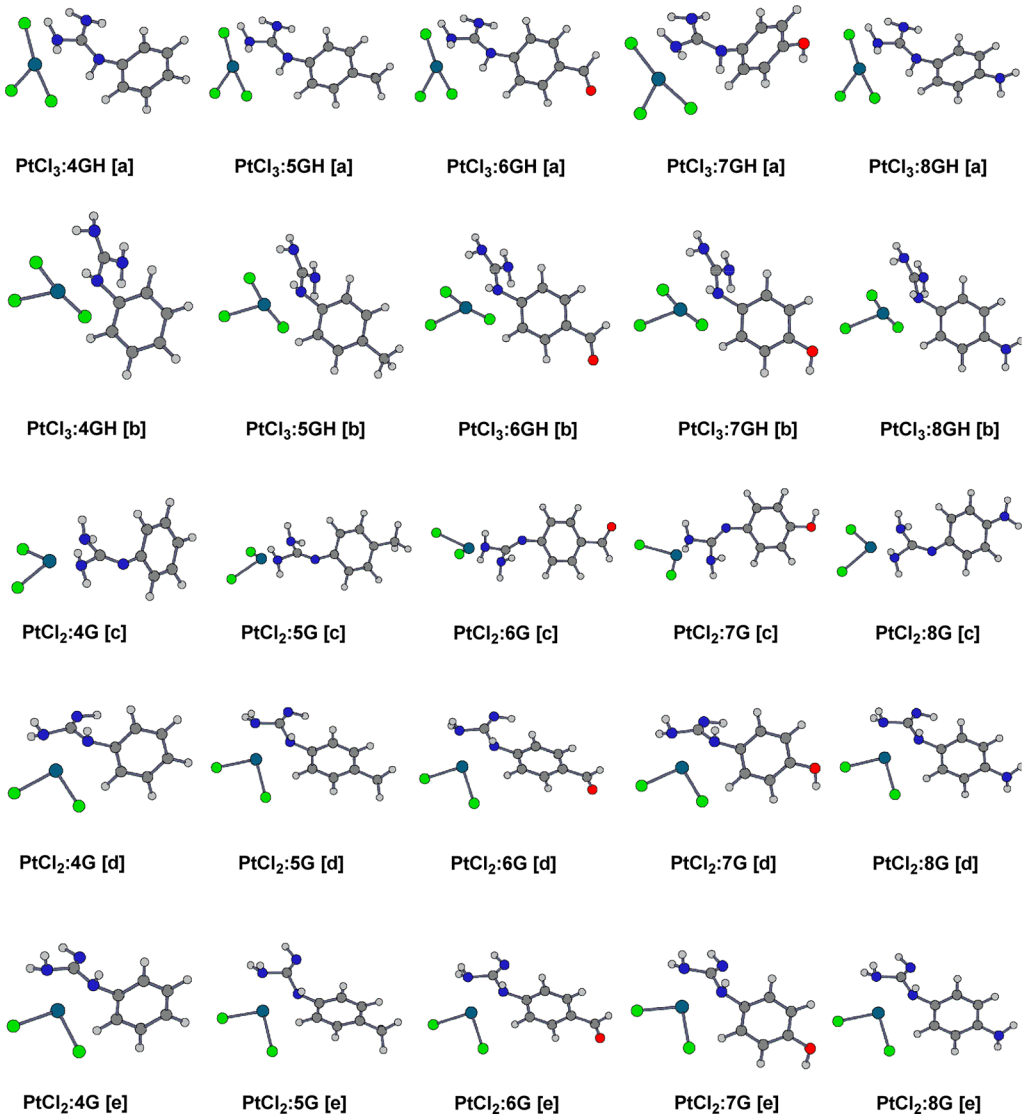

Figure 3. Optimized geometry of the complexes studied in this work at the B3LYP /6-31+G** and LANL2DZ mixed basis set level atom and at the B3LYP/6-31+G** level for the rest of the atoms, in the gas phase.

complexes B3LYP /6-31+G** and LANL2DZ mixed basis set level atom in the gas phase are presented in Figure 3.

The interaction energy of these complexes (E_I, kJ mol^{-1}; Table 1) has been computed as the difference between the total energy of the complexes (E_T; Supporting Information) and the sum of the total energies of the monomers ($E_{Pt} + E_L$; where E_{Pt} is the energy of the either $PtCl_3^-$ or $PtCl_2$, and E_L is the energy of the guanidine/ium ligands {(**4**−**8**)**G**/**GH**[**a**−**e**]}; see Supporting Information), all in their minimum energy conformation. After an exhaustive analysis of the E_I of the complexes shown in Figure 3, the theoretical study predicts a prevalence of complex type [**a**] over [**b**] within the monodentate complexes. However, regarding the bidentate systems (coordinative interactions type [**c**], [**d**], or [**e**]), their E_I values seem to be more influenced by the effect of the aromatic substituent X than for the Pt−N coordination mode.

Specifically, in the monodentate complexes, coordination type [**b**] seems to be less favored than coordination [**a**] for all type of ligands; **PtCl$_3$:8GH** [**b**] (X= NH_2) shows the smallest E_I value and is the least stable of all these complexes, while **PtCl$_3$:6GH** [**a**] (X= CHO) is the strongest of all these complexes with E_I = −349.8 kJ mol^{-1}. Within each type of monodentate coordination [**a**] or [**b**], the effect of the X substituent on the interaction energy follows the same order: NH_2 < CH_3 < OH < H < CHO. However, comparing the E_I of the bidentate complexes, we found that, in all cases and within the same type of coordination, the effect of the X substituent is approximately the opposite of that for the monodentate system, that is, CHO < H < CH_3 < OH < NH_2. Effectively, in these bidentate systems, the poorest stabilized complexes are for X = CHO (**PtCl$_2$:6G** [**c**], −139.7 kJ mol^{-1}; **PtCl$_2$:6G** [**d**], −145.2 kJ mol^{-1}; and **PtCl$_2$:6G** [**e**], −135.1 kJ mol^{-1}); in contrast, when X= NH_2, the resulting complexes (**PtCl$_2$:8G**) are highly stabilized, independent of the mode of Pt coordination.

These results can be justified taking into consideration the electronic effect of both functional groups. In fact, looking at the σ_p Hammet constant values for these chemical groups, the effect on the E_I follows the same order as their constants (NH_2, −0.66; OH, −0.37; CH_3, −0.17; H, 0.0; CHO, 0.42). Thus, while the formyl functionality in the *para* position is an electron-withdrawing group, the amino function donates electron density to the guanidine moiety through the phenyl

dx.doi.org/10.1021/jp504483x | J. Phys. Chem. A 2014, 118, 5540−5547

Table 2. Bond Lengths (Å), Electron Density at the Bond Critical Points and the Corresponding Laplacian (au) for All the Pt−N Bonds Observed in All Complexes Computed at the B3LYP/6-31+G and LANL2DZ Mixed Basis Set**

complex		bond length	ρ-BCP	$\nabla^2\rho$-BCP
$PtCl_3$:4GH [a]	d Pt···N^5	2.16	0.0833	0.381
$PtCl_3$:5GH [a]		2.16	0.0834	0.382
$PtCl_3$:6GH [a]		2.17	0.0831	0.379
$PtCl_3$:7GH [a]		2.17	0.0831	0.380
$PtCl_3$:8GH [a]		2.16	0.0834	0.382
$PtCl_3$:4GH [b]	d Pt···N^8	2.21	0.0758	0.325
$PtCl_3$:5GH [b]		2.22	0.0756	0.324
$PtCl_3$:6GH [b]		2.21	0.0756	0.327
$PtCl_3$:7GH [b]		2.22	0.0752	0.322
$PtCl_3$:8GH [b]		2.22	0.0753	0.321
$PtCl_2$:4G [c]	d Pt···N^5	2.16	0.0885	0.369
	d Pt···N^7	2.16	0.0879	0.368
$PtCl_2$:5G [c]		2.16	0.0887	0.372
		2.16	0.0887	0.372
$PtCl_2$:6G [c]		2.17	0.0858	0.360
		2.17	0.0867	0.362
$PtCl_2$:7G [c]		2.15	0.0892	0.374
		2.16	0.0900	0.375
$PtCl_2$:8G [c]		2.14	0.0916	0.384
		2.14	0.0924	0.384
$PtCl_2$:4G [d]	d Pt···N^5	2.15	0.0908	0.383
	d Pt···N^8	2.20	0.0814	0.322
$PtCl_2$:5G [d]		2.14	0.0909	0.384
		2.20	0.0816	0.322
$PtCl_2$:6G [d]		2.15	0.0901	0.381
		2.21	0.0805	0.320
$PtCl_2$:7G [d]		2.14	0.0912	0.385
		2.21	0.0812	0.320
$PtCl_2$:8G [d]		2.14	0.0912	0.386
		2.21	0.0813	0.319
$PtCl_2$:4G [e]	d Pt···N^5	2.14	0.0917	0.392
	d Pt···N^8	2.18	0.0822	0.318
$PtCl_2$:5G [e]		2.14	0.0912	0.390
		2.20	0.0825	0.321
$PtCl_2$:6G [e]		2.14	0.0906	0.388
		2.21	0.0815	0.320
$PtCl_2$:7G [e]		2.14	0.0916	0.392
		2.20	0.0820	0.319
$PtCl_2$:8G [e]		2.14	0.0917	0.392
		2.20	0.0822	0.318

ring, facilitating the charge transfer between guanidine N atoms and the Pt.

When computing the total energies of the Pt chloride systems (E_{Pt}), we observed a strong effect on their geometry upon complexation. For that reason, we have calculated the relative stabilities of these complexes (E_R) without taking into account E_{Pt}. The relative energy is calculated as the difference between the total energy of the complex (E_T) and the total energy of the guanidine/ium system (E_L), and ΔE_R is the relative energy with respect to the maximum E_R value within those complexes with a common Pt chloride system (E_{Rmax} for [a] and [b]; or E_{Rmax} for [c], [d], and [e]). These ΔE_R values,

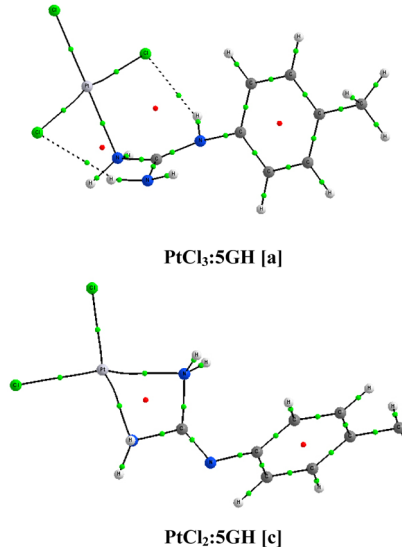

Figure 4. AIM molecular graph of **$PtCl_3$:5GH** [a] and **$PtCl_2$:5GH** [c] complexes showing BCPs between Pt or Cl and Cl, N, or H atoms (small green dots), and ring critical points (RCPs, small red dots).

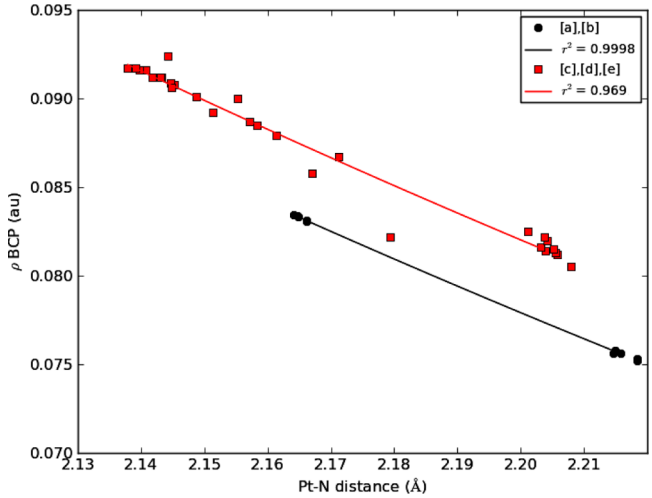

Figure 5. Exponential relationships found between electron density at the BCP (ρ-BCP, au) and the Pt−N distance (Å) for monodentate ([a] and [b], in red squares) and bidentate ([c], [d], and [e], in black circles) complexes.

which represent the stability of these complexes, are presented in Table 1.

Relevant Pt−N bond lengths (Å) found for the *para*-substituted arylguanidine/ium Pt complexes are shown in Table 2. The Pt−N bond lengths computed for all complexes (around 2.14−2.22 Å) are in agreement with those published for structures containing Pt−N bonds,[27−30] although the Pt−N bond corresponding to the exocyclic N atom is longer than the rest of the Pt−N bonds. The geometry around the Pt is planar-square in complexes of type [a] (with Cl−Pt−N angle = 179.7°) and [b] (with Cl−Pt−N angle = 175.5°), while it is different for complexes of type [c], [d], and [e]. For example, in **$PtCl_2$:4G** [c], the NH_2−Pt−NH_2 angle is 65.1°, and for complexes [d] and [e] the NH_2−Pt−NH angle is 64.7° and 65.8°, respectively.

Regarding the topological analysis of the electron density following the AIM approach, bond critical points (BCPs) were

dx.doi.org/10.1021/jp504483x | J. Phys. Chem. A 2014, 118, 5540−5547

Table 3. Orbital Interaction, Second-Order Orbital Energy [$E(2)$, kJ mol^{-1}] and Charge Difference ΔQ_{Pt} (e) of the Pt Model Complexes Studied

complex	orbital interaction	$E(2)$	ΔQ_{Pt}[a]
$PtCl_3$:4GH [a]	LP N^5 → LP* Pt	135.8	−0.528
	LP Pt → LP* C^6	107.7	
$PtCl_3$:5GH [a]	LP N^5 → LP* Pt	135.1	−0.528
	LP Pt → LP* C^6	104.3	
$PtCl_3$:6GH [a]	LP N^5→ LP* Pt	135.1	−0.526
	LP Pt → LP* C^6	121.2	
$PtCl_3$:7GH [a]	LP N^5 → LP* Pt	137.0	−0.532
	LP Pt → LP* C^6	106.1	
$PtCl_3$:8GH [a]	LP N^5 → LP* Pt	137.6	−0.532
	LP Pt → LP* C^6	98.7	
$PtCl_3$:4GH [b]	LP N^8 → LP* Pt	106.7	−0.537
	LP Pt → LP* C^6	152.8	
$PtCl_3$:5GH [b]	LP N^8 → LP* Pt	106.7	−0.536
	LP Pt → LP* C^6	151.1	
$PtCl_3$:6GH [b]	LP N^8 → LP* Pt	104.5	−0.539
	LP Pt → LP* C^6	158.7	
$PtCl_3$:7GH [b]	LP N^8 → LP* Pt	106.0	−0.538
	LP Pt → LP* C^6	148.4	
$PtCl_3$:8GH [b]	LP N^8 → LP* Pt	106.6	−0.535
	LP Pt → LP* C^6	148.1	
$PtCl_2$:4G [c]	LP N^5 → BD* Pt−Cl^3	126.6	−0.380
	LP N^7 → BD* Pt−Cl^2	124.1	
$PtCl_2$:5G [c]	LP N^5 → BD* Pt−Cl^3	128.0	−0.380
	LP N^7 → BD* Pt−Cl^2	126.0	
$PtCl_2$:6G [c]	LP N^5 → BD* Pt−Cl^3	122.9	−0.381
	LP N^7 → BD* Pt−Cl^2	119.8	
$PtCl_2$:7G [c]	LP N^5 → BD* Pt−Cl^3	129.0	−0.380
	LP N^7 → BD* Pt−Cl^2	126.9	
$PtCl_2$:8G [c]	LP N^5 → BD* Pt−Cl^3	134.0	−0.380
	LP N^7 → BD* Pt−Cl^2	131.7	
$PtCl_2$:4G [d]	LP N^5 → BD* Pt−Cl^3	134.2	−0.386
	LP N^8 → BD* Pt−Cl^2	108.2	
$PtCl_2$:5G [d]	LP N^5 → BD* Pt−Cl^3	134.4	−0.385
	LP N^8 → BD* Pt−Cl^2	108.5	
$PtCl_2$:6G [d]	LP N^5 → BD* Pt−Cl^3	133.5	−0.389
	LP N^8 → BD* Pt−Cl^2	106.6	
$PtCl_2$:7G [d]	LP N^5 → BD* Pt−Cl^3	134.7	−0.385
	LP N^8 → BD* Pt−Cl^2	107.8	
$PtCl_2$:8G [d]	LP N^5 → BD* Pt−Cl^3	134.8	−0.384
	LP N^8 → BD* Pt−Cl^2	120.4	
$PtCl_2$:4G [e]	LP N^5 → BD* Pt−Cl^3	133.8	−0.387
	LP N^8 → BD* Pt−Cl^2	109.6	
$PtCl_2$:5G [e]	LP N^5 → BD* Pt−Cl^3	134.1	−0.386
	LP N^8 → BD* Pt−Cl^2	109.9	
$PtCl_2$:6G [e]	LP N^5 → BD* Pt−Cl^3	133.4	−0.390
	LP N^8 → BD* Pt−Cl^2	108.0	
$PtCl_2$:7G [e]	LP N^5 → BD* Pt−Cl^3	134.5	−0.386
	LP N^8 → BD* Pt−Cl^2	108.9	
$PtCl_2$:8G [e]	LP N^5 → BD* Pt−Cl^3	134.8	−0.385
	LP N^8 → BD* Pt−Cl^2	109.1	

[a] ΔQ_{Pt} values are calculated as the difference of the charge of the complex minus that of $PtCl_3^-$ or $PtCl_2$.

found between Pt and the guanidine/ium N atoms (Figure 4). The values of the electron density at those BCPs vary between 0.0752 and 0.0917 au, all in agreement with strong closed-shell interactions.

In the case of type [a] complexes, ρ-BCP values found were 0.0831−0.0834 au, while in type [b] these were slightly smaller 0.0752−0.0758 au. Complexes oftype [c], [d], and [e], in general, showvalues of the electron density at the BCP larger than those of type [a] and [b]. Bidentate complexes with $PtCl_2$ present two slightly different Pt−N bonds; in all the systems, the Pt−N^5 bond shows values of ρ-BCP smaller than that in Pt−N^7 and Pt−N^8 bonds. As a whole, the ρ values found at the BCPs between Pt and guanidine/ium N atoms together with the large and positive values of the Laplacian indicate the metallic nature of these bonds. As in previous studies,[31−36] exponential relationships have been found between the ρ-BCP and the Pt−N distance (Figure 5). As has been pointed out by other authors,[37,38] this type of data can be clustered based on the size of the rings formed by the interacting atoms. In the present work, the data have been divided into two groups: those corresponding to monodentate complexes (type [a] or [b] forming single Pt−N interactions) and those corresponding to bidentate complexes (type [c], [d], or [e]) which form a 4-membered ring with two Pt−N bonds.

The orbital interaction responsible for complexation as well as the charge transferred has been investigated by means of natural bond orbital analysis, and the results are presented in Table 3. The NBO second-order perturbation energy [$E(2)$] at type [a] and [b] complexes reveals orbital interactions between the lone pair of the guanidinium NH_2 or NH groups and the antibonding lone pair of the Pt atom. This study also predicts that a high orbital interaction is established between a lone pair of the Pt atom to the "empty" lone pair of the central C atom of the guanidinium groups. In type [a] complexes, the LP N^5 → LP* Pt (135.1−137.6 kJ mol^{-1}) orbital interaction is higher than the LP Pt → LP* C^6 (98.7−121.2 kJ mol^{-1}). In complexes of type [b], the largest orbital interaction is the later, from Pt to the guanidinium group (LP Pt → LP* C^6 148.1−158.8 kJ mol^{-1}). On the other hand, the most important orbital interactions in the bidentate guanidine complexes ([c], [d], and [e]) are from a lone pair of N^7 or N^8 atoms to the Pt−Cl^2 antibonding orbitals and from a lone pair of N^5 to the Pt−Cl^3 antibonding orbitals, respectively.

The charge transferred from Pt atoms to the guanidine/ium ligands upon complexation is assessed as a difference of the Pt charge from the complex minus the Pt charge from the corresponding isolated $PtCl_3^-$ or $PtCl_2$ moiety. In these systems, Pt bears a positive charge of 0.73 and 0.68 e, respectively. This is consistent with the number of halogen substituents around the Pt atom; the larger the number of Cl atoms, the larger the withdrawing capacity and therefore the smaller negative charge on the Pt atom. Upon complexation in monodenate systems of type [a] and [b], Pt suffers a charge increase of about 0.53−0.54 e, while in type [c], [d], and [e], that increment is smaller, 0.38−0.39 e. This is again consistent with the number of Cl atoms around the Pt; considering that in the isolated $PtCl_3^-$ the metal atom bears a more positive charge than in $PtCl_2$, it is expected that once the complex is formed, the Pt will accept more charge.

In summary, energy, electron density, orbital interaction, and charge-transfer results seem to indicate that the most favorable interaction between a Pt chloride species and a guanidine or guanidinium-containing aromatic system is that established between a guanidinium cation and the $PtCl_3^-$ moiety in a monodentate form of type [a].

Platinum Complexes of the *Bis*-Guanidinium Minor Groove Binders. Once the best Pt···guanidine-like interaction

dx.doi.org/10.1021/jp504483x | J. Phys. Chem. A 2014, 118, 5540−5547

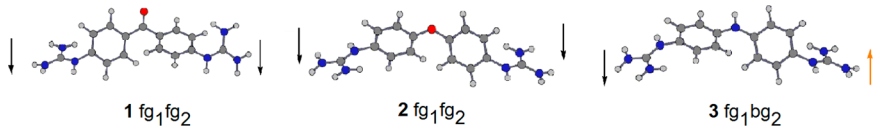

Figure 6. Optimized minimum energy conformations obtained for the *bis*-guanidinium diphenyl derivatives (**1**−**3**) studied at the B3LYP/6-31+G** level in PCM-water phase.

Table 4. Dihedral Angles (Degrees) of the Optimized Compounds Studied at the B3LYP/6-31+G Level in PCM-Water Phase**

compd.	θ_1 (C^1–N^4–C^5–C^6)	θ_2 (C^7–C^8–X^9–C^{10})	θ_3 (C^{11}–C^{10}–X^9–C^8)	θ_4 (C^{15}–N^{14}–C^{13}–C^{12})
1 fg1fg2	−128.2	−25.0	−38.3	−118.6
2 fg1fg2	107.0	−20.8	−54.3	−101.5
3 fg1bg2	102.9	−21.6	−21.6	102.9

was explored, we optimized three different *bis*-guanidinium diaromatic systems with different X linkers (see Figure 1), compounds **1** (X = CO), **2** (X = O), and **3** (X = NH), by computational methods at theoretical level B3LYP/6-31+G**. All of them present four possible geometries, resulting in the same number of diastereoisomers to each system studied. The conformation is determined by the orientation in the space of the guanidinium unit (g1 or g2, as defined in Figure 1) with respect to the phenyl group that supports them. Thus, the notation for the guanidinium group is "b" (orange arrow, Figure 6) when the N^2 or N^{16} atoms from the guanidinium groups are *behind* the plane containing phenyl ring 1 or 2, respectively. The "f" notation (green arrow, Figure 6) is used in those cases where N^2 or N^{16} atoms are in *front* of the corresponding phenyl plane. For all of the *bis*-guanidinum diaromatic systems computed, the minimum energy conformation obtained depends on the phase used in the study (gas or PCM-aqueous solution, see Supporting Information). For all of the **1**−**3** systems the, bg1fg2 geometry corresponds to the minimum energy conformation in the gas phase. However, the minimum energy conformation of **1** (X = CO) and **2** (X = O) using PCM-aqueous solvation show a fg1fg2 orientation with both guanidinium groups in front of their respective phenyl rings, whereas compound **3** (X = NH) shows an fg1bg2 combination as the minimum energy conformation (Figure 6).

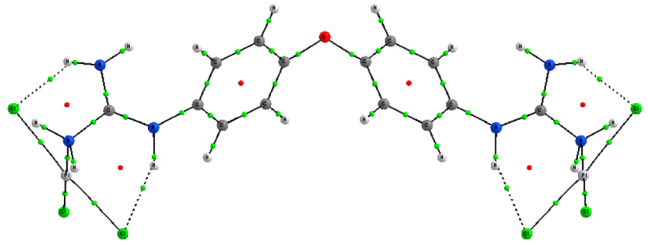

Figure 7. AIM molecular graph of $(PtCl_3)_2$**:2** complex showing BCPs between Pt or Cl and Cl, N, or H atoms (small green dots) and ring critical points (RCPs, small red dots).

It is known that if a compound is prone to interact with a DNA molecule, the interaction energy will be higher when the compound presents a higher planar geometry (coplanarity between both phenyl rings), with respect to other possible conformations.[12] The values of the relevant dihedral angles of molecules **1**−**3** are collected in Table 4. All the complexes show the phenyl rings rotated with respect to each other (see θ_2 and θ_3), and the guanidinium groups are out from the planes that contain the phenyl rings (see θ_1 and θ_4).

Next, the computational study of the corresponding optimal complexes of type [**a**] of **1**, **2**, or **3** with two $PtCl_3^-$ units was pursued, and the optimized geometry, interaction energy, and relative energy difference of those bifunctional monodentate complexes are presented in Table 5. The most stable complex is that with the CO linker followed by that with X = O and then that with X = NH, very similar to the trend followed by the $PtCl_3$**:(4**−**8)GH** [**a**] complexes, in which the most stable complex was that with a CHO group in the *para* position to the guanidinium and the most unstable was that with an NH_2 group.

All Pt−N distances found in the optimized complexes with compounds **1**−**3** are around 1.67 Å, similar to the distances obtained in the type [**a**] complexes with $PtCl_3^-$. In the AIM

Table 5. Interaction Energy (E_I, kJ mol^{-1}), Relative Energy Difference (ΔE_R, kJ mol^{-1}) and Optimized Geometry of $PtCl_3^-$ Complexes of Compounds 1, 2, and 3 Calculated at the B3LYP /6-31+G and LANL2DZ Mixed Basis Set Level Atom and at the B3LYP/6-31+G** Level for the Rest of the Atoms**

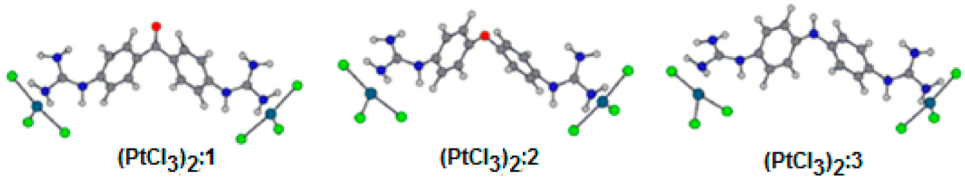

Complex	E_I	ΔE_R
$(PtCl_3)_2$**:1**	-825.8	-24.0
$(PtCl_3)_2$**: 2**	-814.7	-12.9
$(PtCl_3)_2$**:3**	-801.8	0.0

dx.doi.org/10.1021/jp504483x | *J. Phys. Chem. A* 2014, 118, 5540−5547

analysis of the three complexes, BCPs were found between the Pt atoms and guanidinium N atoms (Figure 7). The electron density found at the BCPs is 0.0827−0.0830 au in all cases, and the corresponding Laplacian ranges between 0.378 and 0.379 au. As it occurs in the model complexes, those values are in agreement with the existence of a metallic bond between Pt and N atoms.

Regarding the NBO analysis of complexes **1**−**3** (Table 6), $E(2)$ values and charge increase on the Pt atoms have been found in these *bis*-guanidinium diaromatic systems similar to those shown by the **$PtCl_3$:(4−8)G** [a] and [b] complexes. This confirms that in such complexes the orbital interaction and charge transfer are governed by the coordination around the metal rather than the substituent considered.

Table 6. Orbital Interaction, Second-Order Orbital Energy [$E(2)$, kJ mol^{-1}] and Charge Difference ΔQ_{Pt} (e) of the *Bis*-guanidinium Diaromatic Pt Complexes Studied

complex	orbital interaction	$E(2)$	ΔQ_{Pt}
$(PtCl_3)_2$:1	LP N^3→ LP* Pt	135.4	−0.527
	LP N^{17}→ LP* Pt	135.3	
	LP Pt→ LP* C^1	123.8	
	LP Pt→ LP* C^{15}	123.8	
$(PtCl_3)_2$:2	LP N^3→ LP* Pt	118.1	−0.530
	LP N^{17}→ LP* Pt	118.2	
	LP Pt→ LP* C^1	135.7	
	LP Pt→ LP* C^{15}	135.7	
$(PtCl_3)_2$:3	LP N^3→ LP* Pt	136.1	−0.529
	LP N^{17}→ LP* Pt	136.1	
	LP Pt→ LP* C^1	114.9	
	LP Pt→ LP* C^{15}	114.9	

CONCLUSIONS

With the aim of understanding the complexation between Pt and the guanidine or guanidinium moiety, we have calculated the complexes of model *N*-phenylguanidine/ium derivatives (**4**−**8**) with $PtCl_3^-$ and $PtCl_2$ in different coordinating modes (mono- and bidentate) with different N atoms of the guanidine/ium moiety, using the B3LYP/6-31+G** and LAN2DZ mixed basis set at the gas phase.

Interaction energies (calculated as the difference between the energies of the complexes and those of the Pt systems and guanidine/ium systems) and relative energies (calculated considering only the total energies of the complex and guanidine/ium moiety) were calculated for all the complexes studied.

Analysis of the electron density by means of the AIM approach and examination of the orbital interactions and charge transferred by means of NBO calculations together with the interaction energy calculated all indicate that the most stable type of complex is the type [a] coordination, which is a monodentate interaction with the guanidinium cation established through one of the NH_2 groups of the cation.

On the basis of these results, we optimized the structure of three *bis*-guanidinium diaromatic systems (**1**−**3**) developed in our group as DNA minor groove binders and then their complexation with $PtCl_3^-$ in a coordination type [a]. Interaction and relative difference energies as well as AIM and NBO analyses were carried out indicating that the formation of Pt complexes of these minor groove binders is favorable and will produce stable monodentate coordinated systems. Therefore, when they are prepared experimentally, we should expect monodentate Pt complexes of our guanidine-based minor groove binders.

ASSOCIATED CONTENT

Supporting Information

Total energies and AIM molecular graphs of the **$PtCl_3$:(4−8)GH** [a,b] and **$PtCl_2$:(4−8)G** [c,d,e] and of the Pt complexes of the minor groove binders **1**−**3** optimized at B3LYP/6-31+G** and LANL2DZ mixed basis set. This material is available free of charge via the Internet at http://pubs.acs.org.

AUTHOR INFORMATION

Corresponding Author

*Phone: (+353)18963731. Fax: (+353)16712826. E-mail: rozasi@tcd.ie.

Notes

The authors declare no competing financial interest.

ACKNOWLEDGMENTS

This research was supported by Science Foundation Ireland (Project Reference: SFI-CH3060). P.O'S. thanks SFI for generous funding. M.M.-L. thanks the Ministerio de Educación, Cultura y Deporte of Spain for her fellowship (Reference: MHE2011-00211). G.S.-S. thanks the Human Frontier Science Program (Project Reference: LT001022/2013-C) for the support. We are indebted to Prof. Ibon Alkorta from the Instituto de Quimica Medica (CSIC) for the AIM analysis.

REFERENCES

(1) Galanski, M.; Jakupec, M. A.; Keppler, B. K. Update of the Preclinical Situation of Anticancer Platinum Complexes: Novel Design Strategies and Innovative Analytical Approaches. *Curr. Med. Chem.* **2005**, *12*, 2075−2094 and references therein..

(2) Kelland, L. The Resurgence of Platinum-Based Cancer Chemotherapy. *Nat. Rev. Cancer* **2007**, *7*, 573−584.

(3) Ruhayel, R. A.; Moniodis, J. J.; Yang, X.; Kasparkova, J.; Brabec, V.; Berners-Price, S. J.; Farrell, N. P. Factors Affecting DNA-DNA Interstrand Cross-Links in the Antiparallel 3′-3′ Sense: A Comparison with the 5′-5′ Directional Isomer. *Chem.—Eur. J.* **2009**, *15*, 9365−9374.

(4) Navarro, M.; Higuera-Padilla, A. R.; Arsenak, M.; Taylor, P. Synthesis, Characterization, DNA Interaction Studies and Anticancer Activity of Platinum−Clotrimazole Complexes. *Transition Met. Chem. (Dordrecht, Neth.)* **2009**, *34*, 869−875.

(5) Taleb, R. I.; Jaramillo, D.; Wheate, N. J.; Aldrich-Wright, J. R. Synthesis of DNA-Sequence-Selective Hairpin Polyamide Platinum Complexes. *Chem.—Eur. J.* **2007**, *13*, 3177−3186.

(6) Choudhury, J. R.; Bierbach, U. Characterization of the Bisintercalative DNA Binding Mode of a Bifunctional Platinum Acridine Agent. *Nucleic Acids Res.* **2005**, *33*, 5622−5632.

(7) Baruah, H.; Barry, C. G.; Bierbach, U. Platinum-Intercalator Conjugates: From DNA-Targeted Cisplatin Derivatives to Adenine Binding Complexes as Potential Modulators of Gene Regulation. *Curr. Top. Med. Chem.* **2004**, *4*, 1537−1549.

(8) Griffith, D.; Morgan, M. P.; Marmion, C. J. A Novel Anti-Cancer Bifunctional Platinum Drug Candidate with Dual DNA Binding and Histone Deacetylase Inhibitory Activity. *Chem. Commun. (Cambridge, U.K.)* **2009**, 6735−6737.

(9) Dardonville, C.; Goya, P.; Rozas, I.; Alsasua, A.; Martín, M. S.; Borrego, M. J. New Aromatic Iminoimidazoline Derivatives as α_1-Adrenoceptor Antagonists: A Novel Synthetic Approach and Pharmacological Activity. *Bioorg. Med. Chem.* **2000**, *8*, 1567−1577.
(10) Rodriguez, F.; Rozas, I.; Kaiser, M.; Brun, R.; Nguyen, B.; Wilson, W. D.; Garcia, R. N.; Dardonville, C. New Bis(2-aminoimidazoline) and Bisguanidne DNA Minor Groove Binders with Potent in Vivo Antitrypanosomal and Antiplasmodial Activity. *J. Med. Chem.* **2008**, *51*, 909−923.
(11) Nagle, P. S.; Rodriguez, F.; Kahvedžić, A.; Quinn, S. J.; Rozas, I. Non-Symmetrical Diaromatic Guanidinium/2-Aminoimidazolinium Derivatives: Synthesis and DNA Affinity. *J. Med. Chem.* **2009**, *52*, 7113−7121.
(12) Nagle, P. S.; Rodriguez, F.; Quinn, S. J.; O'Donovan, D. H.; Kelly, J. M.; Nguyen, B.; Wilson, W. D.; Rozas, I. Biophysical Studies on the DNA Interaction with Non-Symmetrical Guanidinium/2-Aminoimidazolinium Derivatives. *Org. Biomol. Chem.* **2010**, *8*, 5558−5567.
(13) Baruah, H.; Rector, L. C.; Monnier, S. M.; Bierbach, U. Mechanism of Action of Non-Cisplatin Type DNA-Targeted Platinum Anticancer Agents: DNA Interactions of Novel Acridinylthioureas and their Platinum Conjugates. *Biochem. Pharmacol.* **2002**, *64*, 191−200.
(14) Baruah, H.; Bierbach, U. Biophysical Characterization and Molecular Modeling of the Coordinative-Interactive DNA Monoadduct of a Platinum-Acridinylthiourea Agent in a Site-Specifically Modified Dodecamer. *J. Biol. Inorg. Chem.* **2004**, *9*, 335−344.
(15) Corson, T. W.; Aberle, N.; Crews, C. M. Design and Applications of Bifunctional Small Molecules: Why Two Heads are Better than One. *ACS Chem. Biol.* **2008**, *3*, 677−692.
(16) Picazo, O.; Alkorta, I.; Elguero, J.; Sundberg, M. R.; Valo, J. Bonding Properties Related with Chiral Discrimination in Dinuclear Metal Complexes of Group 10. *Eur. J. Inorg. Chem.* **2007**, 324−332.
(17) Picazo, O.; Alkorta, I.; Elguero, J.; Sundberg, M. R.; Valo, J.; Zborowski, K. Chiral Distinction in Square Planar Pt and Pd Complexes of 2,2′-Bipyridine Derivatives. *Struct. Chem.* **2009**, *20*, 557−563.
(18) Miehlich, B.; Savin, A.; Preuss, H. Results Obtained with the Correlation Energy Density Functionals of Becke and Lee, Yang and Parr. *Chem. Phys. Lett.* **1989**, *157*, 200−206.
(19) Frisch, M. J.; Trucks, G. W.; Schlegel, H. B.; Scuseria, G. E.; Robb, M. A.; Cheeseman, J. R.; Scalmani, G.; Barone, V.; Mennucci, B.; Petersson, G. A.; Nakatsuji, H.; Caricato, M.; Li, X.; Hratchian, H. P.; Izmaylov, A. F.; Bloino, J.; Zheng, G.; Sonnenberg, J. L.; Hada, M.; Ehara, M.; Toyota, K.; Fukuda, R.; Hasegawa, J.; Ishida, M.; Nakajima, T.; Honda, Y.; Kitao, O.; Nakai, H.; Vreven, T.; Montgomery, J. A., Jr.; Peralta, J. E.; Ogliaro, F.; Bearpark, M.; Heyd, J. J.; Brothers, E.; Kudin, K. N.; Staroverov, V. N.; Kobayashi, R.; Normand, J.; Raghavachari, K.; Rendell, A.; Burant, J. C.; Iyengar, S. S.; Tomasi, J.; Cossi, M.; Rega, N.; Millam, N. J.; Klene, M.; Knox, J. E.; Cross, J. B.; Bakken, V.; Adamo, C.; Jaramillo, J.; Gomperts, R.; Stratmann, R. E.; Yazyev, O.; Austin, A. J.; Cammi, R.; Pomelli, C.; Ochterski, J. W.; Martin, R. L.; Morokuma, K.; Zakrzewski, V. G.; Voth, G. A.; Salvador, P.; Dannenberg, J. J.; Dapprich, S.; Daniels, A. D.; Farkas, Ö.; Foresman, J. B.; Ortiz, J. V.; Cioslowski, J.; Fox, D. J. *Gaussian 09*, revision D.01; Gaussian, Inc.: Wallingford, CT, 2009.
(20) Wadt, W. R.; Hay, P. J. *Ab Initio* Effective Core Potentials for Molecular Calculations. Potentials for Main Group Elements Na to Bi. *J. Chem. Phys.* **1985**, *82*, 284−298.
(21) Hay, P. J.; Wadt, W. R. *Ab Initio* Effective Core Potentials for Molecular Calculations. Potentials for K to Au including the Outermost Core Orbitals. *J. Chem. Phys.* **1985**, *82*, 299−310.
(22) Frisch, M. J.; Pople, J. A.; Binkley, J. S. Self-Consistent Molecular Orbital Methods 25. Supplementary Functions for Gaussian Basis Sets. *J. Chem. Phys.* **1984**, *80*, 3265−3269.
(23) Reed, A. E.; Curtiss, L. A.; Weinhold, F. Intermolecular Interactions From a Natural Bond Orbital, Donor−Acceptor Viewpoint. *Chem. Rev. (Washington, DC, U.S.)* **1988**, *88*, 899−926.
(24) Bader, R. F. W. *Atoms in Molecules: A Quantum Theory*; Clarendon Press: Oxford, 1990.
(25) Popelier, P. L. A. *Atoms in Molecules. An Introduction*; Prentice Hall: Harlow, England, 2000.
(26) Keith, T. A. AIMAll, version 11.10.16; TK Gristmill Software: Overland Park, KS, 2011; aim.tkgristmill.com.
(27) Bai, F. Q.; Liu, T.; Zhou, X.; Zhang, J. P.; Zhang, H. X. Theoretical Computational Studies on Electronic Structures, Spectroscopic Properties and Nitrogen Heteroatom Effect of a Species of Asymmetrical Diimine Ligand Platinum(II) Complexes. *J. Theor. Comput. Chem.* **2009**, *8*, 603−613.
(28) Gushchin, P. V.; Kuznetsov, M. L.; Haukka, M.; Wang, M. J.; Gribanov, A. V.; Kukushkin, V. Y. A Novel Reactivity Mode for Metal-Activated Dialkylcyanamide Species: Addition of *N,N′*-Diphenylguanidine to a *cis*-$(R_2NCN)_2Pt^{II}$ Center Giving an Eight-Membered Chelated Platinaguanidine. *Inorg. Chem.* **2009**, *48*, 2583−2592.
(29) Aitken, D. J.; Albinati, A.; Gautier, A.; Husson, H. P.; Morgant, G.; Nguyen-Huy, D.; Kozelka, J.; Lemoine, P.; Ongeri, S.; Rizzato, S.; Viossat, B. Platinum(II) and Palladium(II) Complexes with *N*-Aminoguanidine. *Eur. J. Inorg. Chem.* **2007**, 3327−3334.
(30) Xu, X.; Kua, J.; Periana, R. A.; Goddard, W. A., III Structure, Bonding, and Stability of a Catalytica Platinum(II) Catalyst: A Computational Study. *Organometallics* **2003**, *22*, 2057−2068.
(31) Alkorta, I.; Elguero, J. Fluorine-Fluorine Interactions: NMR and AIM Analysis. *Struct. Chem.* **2004**, *15*, 117−120.
(32) Tang, T. H.; Deretey, E.; Knak Jensen, S. J.; Csizmadia, I. G. Hydrogen Bonds: Relation Between Lengths and Electron Densities at Bond Critical Points. *Eur. Phys. J. D* **2006**, *37*, 217−222.
(33) Vener, M. V.; Manaev, A. V.; Egorova, A. N.; Tsirelson, V. G. QTAIM Study of Strong H-Bonds with the O−H···A Fragment (A = O, N) in Three-Dimensional Periodical Crystals. *J. Phys. Chem. A* **2007**, *111*, 1155−1162.
(34) Sanchez-Sanz, G.; Alkorta, I.; Elguero, J. Theoretical Study of the HXYH Dimers (X, Y= O, S, Se). Hydrogen Bonding and Chalcogen-Chalcogen Interactions. *Mol. Phys.* **2011**, *109*, 2543−2542.
(35) Sanchez-Sanz, G.; Trujillo, C.; Alkorta, I.; Elguero, J. Intermolecular Weak Interactions in HTeXH Dimers (X = O, S, Se, Te): Hydrogen Bonds, Chalcogen-Chalcogen Contacts and Chiral Discrimination. *ChemPhysChem* **2012**, *13*, 496−503.
(36) Blanco, F.; Kelly, B.; Sanchez-Sanz, G.; Alkorta, I.; Rozas, I.; Elguero, J. Non-Covalent Interactions: Complexes of Guanidinium with DNA and RNA Nucleobases. *J. Phys. Chem. B* **2013**, *11*, 11608−11616.
(37) Solimannejad, M.; Massahi, S.; Alkorta, I. Glyoxal Oligomers: A Computational Study. *Int. J. Quantum Chem.* **2011**, *111*, 3057−3069.
(38) Azofra, L. M.; Quesada-Moreno, M. M.; Alkorta, I.; Aviles-Moreno, J. R.; Lopez-Gonzalez, J. J.; Elguero, J. Carbohydrates in the Gas Phase: Conformational Preference of D-Ribose and 2-Deoxy-D-ribose. *New J. Chem.* **2014**, *38*, 529−538.